Studies on solid state reactions of atomic layer deposited thin films of lithium carbonate with hafnia and zirconia

Mäntymäki, Miia

2019-03

Mäntymäki , M , Atosuo , E , Heikkilä , M J , Vehkamäki , M , Mattinen , M , Mizohata , K , Räisänen , J , Ritala , M & Leskelä , M 2019 , ' Studies on solid state reactions of atomic layer deposited thin films of lithium carbonate with hafnia and zirconia ' , Journal of vacuum science & technology : an official journal of the American Vacuum Society , vol. 37 , no. 2 , 020929 . https://doi.org/10.1116/1.5081494

http://hdl.handle.net/10138/310948
https://doi.org/10.1116/1.5081494

unspecified
acceptedVersion

Studies on solid state reactions of atomic layer deposited thin films of lithium carbonate with hafnia and zirconia

Running title: Studies on solid state reactions of ALD Li_2CO_3 with HfO_2 and ZrO_2

Running Authors: Mäntymäki et al.

Miia Mäntymäki[a), b)], Elisa Atosuo, Mikko J. Heikkilä, Marko Vehkamäki, Miika Mattinen, Mikko Ritala, Markku Leskelä

Department of Chemistry, University of Helsinki, P.O. Box 55, FI-00014 Helsinki, Finland

a) Current address: Department of Chemistry and Materials Science, School of Chemical Engineering, Aalto University, P.O. Box 16100, FI-00076 AALTO, Finland

Kenichiro Mizohata, Jyrki Räisänen

Department of Physics, University of Helsinki, P.O. Box 43, FI-00014 Helsinki, Finland

b) Electronic mail: miia.mantymaki@aalto.fi

In this paper, results on the solid state reactions of atomic layer deposited Li_2CO_3 with HfO_2 and ZrO_2 are reported. A Li_2CO_3 film was deposited on top of hafnia and zirconia, and the stacks were annealed at various temperatures in air to remove the carbonate and facilitate lithium diffusion into the oxides. It was found that Li^+ ions are mobile in hafnia and zirconia at high temperatures, diffusing to the film-substrate interface and forming silicates with the Si substrate during heating. Based on grazing incidence X-ray diffraction (GIXRD) experiments, no changes in the oxide phases take place during this process. Field emission scanning electron microscopy (FESEM) images reveal that some surface defects are formed on the transition metal oxide surfaces during lithium diffusion.

We also show that lithium can diffuse through hafnia and react with a potential lithium-ion battery electrode material TiO_2 residing below the HfO_2 layer, forming Li_2TiO_3.

I. INTRODUCTION

Hafnium and zirconium oxides are well-known high-κ materials (≈ 30 for HfO_2, ≈ 25 for ZrO_2),[1] useful for MOSFETs and memory devices.[2] Due to their high electrical resistivity, these oxides could prove useful also in all-solid-state lithium-ion batteries as electrolyte materials. However, electrolyte materials are also required to have a high enough lithium-ion conductivity to be useful. The commonly used solid electrolyte LiPON shows Li-ion conductivities between 10^{-6}–10^{-8} S/cm.[3] With the emergence of ever smaller, 3D-structured batteries, geometric reasons could permit the utilization of even somewhat lower ionic conductivities in battery materials. Even though the utilization of hafnia and zirconia as electrolytes in lithium-ion batteries has not been studied as such, some experiments in this area have already been done.[4,5] For example, it has been reported that ultrathin HfO_2 layers can be used to protect SnO_2 nanoparticle anodes, resulting in an improved electrochemical operation of the anode.[4] Even after 200 cycles of HfO_2 (growth rate ≈ 1 Å/cycle) the battery performance is improved, without a loss in diffusion kinetics. These results indicate that at least through thin layers of HfO_2, lithium diffusion is fast enough for battery application. In addition, simple lithium-ion diffusion into ZrO_2 has also been studied.[5] It was found that monoclinic ZrO_2 is a poor lithium-ion conductor and that lithium diffusivity decreases as the amount of Li^+ in the oxide increases.

In this paper, we have studied the interaction of Li_2CO_3 thin films with HfO_2 and ZrO_2 thin films. Previously we have shown that it is possible to form lithium transition metal oxide thin films from lithium carbonate and metal oxides.[6] In the current experiments our goal was to study lithium diffusion into hafnia and zirconia during heating. In addition, we hoped to find out whether lithium hafnates or zirconates could be formed in this manner. Hafnium oxide does not have many well-known lithium containing phases, although at least the structures of two crystalline lithium hafnium oxides are known in the literature, namely Li_2HfO_3 and Li_8HfO_6.[7,8] Lithium hafnate Li_2HfO_3 can be used, for example, as a scintillator material.[9] $Li_6Hf_2O_7$ has also been reported, but very little information on this material is given. However, based on solid-state Li NMR studies this material was concluded to be a poor Li-ion conductor.[10] Lithium zirconates, on the other hand, are much better known in materials science.[11–15] Li_2ZrO_3 has been reported to be a possible tritium breeding material for future fusion reactors.[14] In addition, it can be used to protect lithium-ion battery cathode materials,[11,12] and its application as an anode material in lithium-ion batteries has also been studied.[13] Doped Li_8ZrO_6, on the other hand, has been suggested as a possible cathode material for Li-ion batteries.[15,16]

II. EXPERIMENTAL

A. Film deposition

Li_2CO_3 thin films were deposited in an ASM Microchemistry F-120 hot-wall flow-type ALD reactor onto ZrO_2 and HfO_2 thin films. These films had been deposited by ALD onto single-crystalline silicon wafers using a heteroleptic zirconium precursor and water,[17] and TEMAH (tetrakis(ethylmethylamino)hafnium) and water.[1] Lithd (Volatec oy) and ozone, generated by a Wedeco GmbH Modular 4 HC ozone generator, were used as precursors for the Li_2CO_3 depositions as previously described in the literature.[18] The ozone flow rate was 30 L/h and the concentration was 100 g/Nm^3. Lithd was evaporated inside the reactor at 192 °C at a pressure of approximately 5 mbar. The pulse time for Lithd was 1.5 s with a 2 s purge, and ozone was pulsed for 2.5 s with a 3.5 s purge time. The pulsing of the lithium precursor was done by inert gas valving, with gaseous N_2 as the pulse and purge gas. The N_2, obtained from liquid N_2, had as an impurity less than 3 ppm of H_2O and O_2 each. All the Li_2CO_3 deposition experiments were done at 225 °C.

B. Film characterization

A muffle furnace was used for the annealing of the films. All annealing experiments were done in air with a maximum heating rate of approx. 9 °C/min.

The crystallinity of the films was studied by grazing incidence X-ray diffraction (GIXRD) measurements using a PANalytical X'Pert Pro MPD X-ray diffractometer. *In situ* high temperature XRD (HTXRD) measurements were also conducted with an Anton-

Paar HTK1200N oven. The morphology of the films before and after annealing was studied by field emission scanning electron microscopy with a Hitachi S4800 FESEM instrument. For the FESEM imaging, the samples were coated with approximately 3 nm of Au/Pd by sputtering. No coating was used in the cross-sectional FESEM analyses. Transmission electron microscope (TEM) specimens were prepared using standard focused ion beam (FIB) lift-out procedures. Bright-field TEM images were taken with a FEI Tecnai F20 microscope operated at 200 kV.

Surface roughness was quantified with atomic force microscopy (AFM) using a Veeco Multimode V instrument. Tapping mode images were captured in air using silicon probes with nominal tip radius of 10 nm and nominal spring constant of 5 N/m (Tap150 from Bruker). Images were flattened to remove artefacts caused by sample tilt and scanner bow. Film roughness was calculated as a root-mean-square value (R_q).

The composition of the films was studied with time-of-flight elastic recoil detection analysis (ToF-ERDA). The ToF-ERDA measurements were performed with 50 MeV ^{127}I and 40 MeV ^{79}Br beams from the 5 MV EGP-10-II tandem accelerator at the University of Helsinki.[19] The detection angle was 40° and the sample was tilted 15° relative to the beam direction.

III. RESULTS AND DISCUSSION

A. HfO_2 films as substrates

To study whether lithium containing hafnium oxides could be made by similar solid state reactions as we have reported for Li_2TiO_3, $LiTaO_3$ and $LiNbO_3$,[6] a 50 nm hafnium oxide film was covered with 3000 cycles of atomic layer deposited Li_2CO_3 and the resulting stack was subjected to a high-temperature XRD measurement (Figure 1). In the temperature range studied no crystalline lithium hafnate phases formed. At 565 °C peaks belonging to Li_2CO_3 have disappeared. At the same time, a peak appears at 2θ = 22.2°. The peak is difficult to index, but it could belong to a lithium silicate phase Li_4SiO_4.[20] Hafnium oxide remains monoclinic during heating. At 655 °C orthorhombic lithium silicate Li_2SiO_3 has formed. At the same time, the peak at 22.2° has decreased, possibly indicating a shift from a metastable silicate to a more stable one.

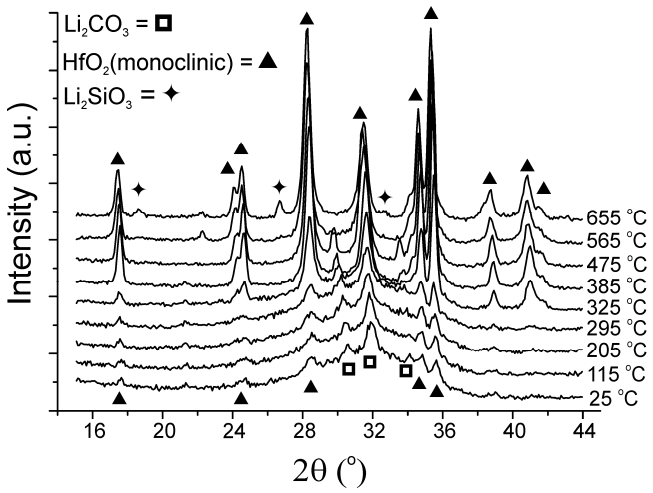

FIG. 1. High temperature X-ray diffractograms of a 3000 cycle Li_2CO_3 film deposited onto 50 nm HfO_2. The annealing was done in air. Patterns: Li_2CO_3 = PDF 22–1141, JCPDS-ICDD, HfO_2 = PDF 34–0104, JCPDS-ICDD, Li_2SiO_3 = PDF 29–0828, JCPDS-ICDD.

For comparison with previous results on other materials,[6] the Li_2CO_3/HfO_2-stack was annealed in air at 650 °C for 2 hours and studied with grazing incidence X-ray diffraction at room temperature (Figure 2). As with the HTXRD-measurement, no Li_2CO_3 or lithium hafnates could be seen after the annealing, with HfO_2 remaining monoclinic. For the HfO_2 layer, the unit cell parameters change 0.2–0.4% upon annealing, with a 0.05 degree change in the β-angle. The literature values for these parameters for the monoclinic HfO_2 lie between the results for the as-deposited and the annealed film, meaning that the actual change in the HfO_2 structure is smaller than 0.4% despite lithium diffusing through the film. A small increase in the crystallite size can be deduced from the results. Based on the wide peaks visible especially in the as-deposited

HfO_2 films, the hafnia crystallites reside in an amorphous oxide matrix. After annealing, Li_2SiO_3 is present in the stack, with no indication of other silicate phases.

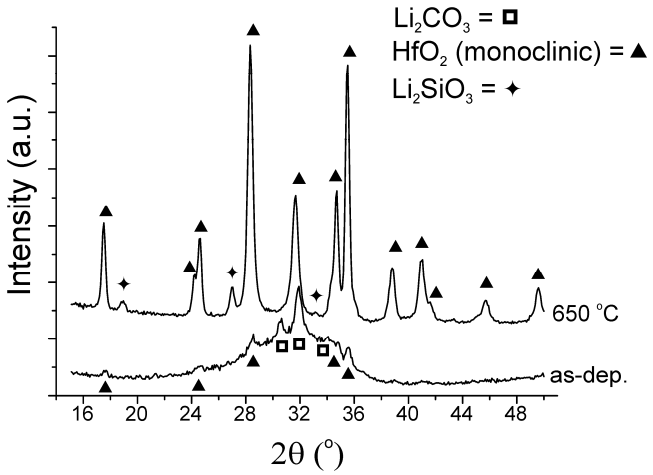

FIG. 2. X-ray diffractograms of a 3000 cycle Li_2CO_3 film deposited onto 50 nm HfO_2 measured as-deposited and after annealing in air at 650 °C for 2 hours. Patterns: Li_2CO_3 = PDF 22–1141, JCPDS-ICDD, HfO_2 = PDF 34–0104, JCPDS-ICDD, Li_2SiO_3 = PDF 29–0828, JCPDS-ICDD.

The films were imagined with FESEM to study their morphology (Figure 3). The as-deposited film showed large platelets on the surface, as is common for Li_2CO_3 films.[18] After the annealing the film showed much smaller, column-like crystallites, and a smoother surface in general, somewhat similarly to titanium oxide films reacted with Li_2CO_3 in our previous study.[6] Atomic layer deposited HfO_2 has been reported to show column-like crystallites after annealing.[21] The change in roughness was quantified with AFM measurements (Figure 4). For the as-deposited film, the rms roughness was as high as 47 nm, with large platelets comprising the surface. After annealing, the roughness of

the film stack decreased to 2.9 nm, which is a typical value for polycrystalline ALD HfO_2 films.[1]

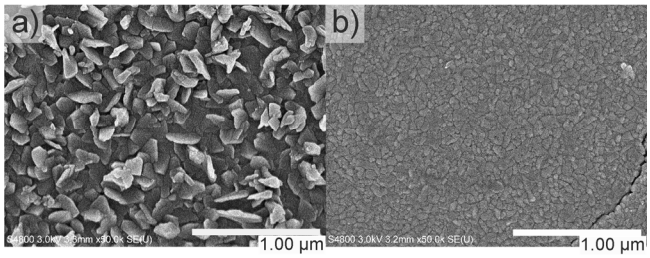

FIG. 3. FESEM images of 3000 cycles of Li_2CO_3 deposited by ALD onto 50 nm of HfO_2, before (a) and after (b) annealing in air at 650 °C.

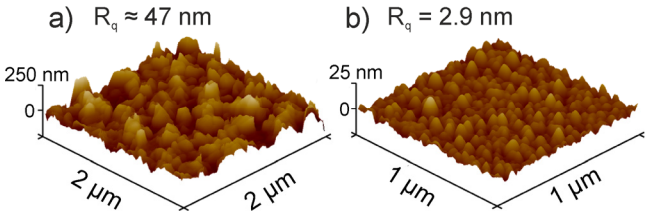

FIG. 4. AFM images of Li_2CO_3/HfO_2-stacks before (a) and after (b) annealing in air at 650 °C.

In the FESEM images, the annealed film showed some cracking on the surface. This differs from the results obtained for other films studied previously in this same manner.[6] One explanation for the surface defects could be the reaction with the silicon substrate, which could cause strain in the HfO_2 film. Some damage could also be caused by carbon dioxide leaving the film structure, even though this type of damage was not

evident in the films forming intermediate lithium transition metal oxide phases. In addition, adhesion problems cannot be completely ruled out, as the samples needed to be cut for the FESEM imaging.

ToF-ERDA measurements revealed that the as-deposited film was close to stoichiometric HfO_2 and Li_2CO_3 (Table I). After annealing the film composition was approximately "Li_2HfO_6", indicating a large excess of oxygen. This excess could be explained by the silicate formation during annealing. Possibly some additional SiO_2 is forming during annealing as a result of the high oxygen diffusivity in HfO_2,[22] and the forming silicon dioxide is further forming silicates. In addition to the lithium silicate seen in the XRD measurements, possibly also some hafnium silicates are forming: a hafnium silicate interfacial layer has been reported to form during annealing of ultra-thin HfO_2 layers on silicon.[23] The ToF-ERDA depth profiles corroborate the XRD results in that lithium is indeed concentrated on the film – Si substrate interface after the annealing (Figure 5). Only a small amount of lithium is incorporated into the HfO_2 film. Moreover, unlike most lithium containing systems, lithium is not concentrated on the outermost film surface.[24,25]

TABLE I. ToF-ERDA results (at%) of a 3000 cycle Li_2CO_3 film deposited onto 50 nm HfO_2 and measured as-deposited and after annealing at 650 °C for 2 h in air.

	Li_2CO_3 / HfO_2 as-deposited	**Li_2CO_3 / HfO_2 after anneal at 650 °C**
Li	18.9±0.4	22.0±0.4
Hf	11.5±0.1	10.9±0.2
O	56.1±0.5	63.8±0.5
C	9.7±0.2	0.94±0.07
H	2.5±0.5	2.2±0.5
F	1.25±0.07	0.07±0.03
Na	0.06±0.03	<0.02
Elemental ratios	Assuming stoichiometric HfO_2: Li:C:O = 1.95 : 1 : 3.41	Li : Hf : O = 2.0 : 1.0 : 5.9

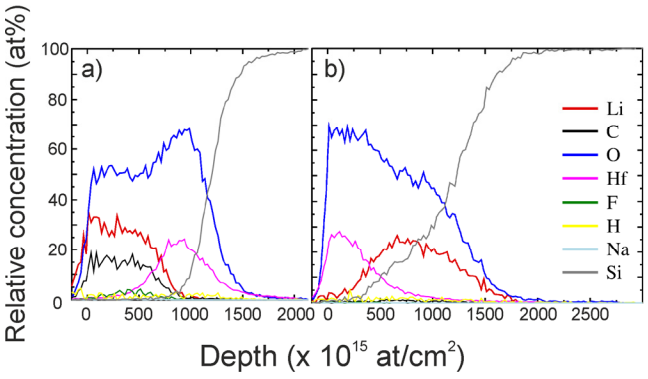

FIG. 5. ToF-ERDA depth profiles of a Li_2CO_3/HfO_2 film stack before (a) and after annealing in air at 650 °C (b).

To study whether it would be possible to mix the lithium ions with hafnia more completely and without silicate formation, a series of annealing experiments was made. 3000 cycles of Li_2CO_3 was deposited onto 50 nm of HfO_2, and the stack was annealed in air at 300, 400, 500 and 600 °C for 2 hours. In addition, samples were annealed at 300 °C for 4 hours to see whether a longer annealing time could make a difference in the lithium diffusion. After annealing the films were studied both with GIXRD and ToF-ERDA and the results are collected in Figures 6 and 7. From Fig. 6 it is apparent that crystalline lithium carbonate has reacted completely only after annealing at 600 °C. Comparing this information with Fig. 7 reveals that the lower temperatures used were not enough to promote full mixing of lithium and hafnium oxide. Some migration has occurred already at 400 and 500 °C, but in these films lithium is still strongly enriched on the stack surface as the carbonate. In addition, the amount of carbon has not decreased in these samples. Only after annealing at 600 °C has the carbonate been decomposed, and lithium has diffused through the hafnia film to the silicon substrate interface. During the annealing the carbon impurities were removed from the film. However, this change was accompanied by an increase in the amount of hydrogen, from 2.2 at% at 500 °C to 6.3 at% at 600 °C. This could be explained by LiOH formation caused by lithium enrichment on the film surface and reaction with ambient air, similarly to the $LiTaO_3$ sample studied previously.[6] Interestingly, despite the large amount of lithium in the silicon substrate surface after the annealing at 600 °C, no crystalline lithium silicates can be found in Fig. 6 at this temperature.

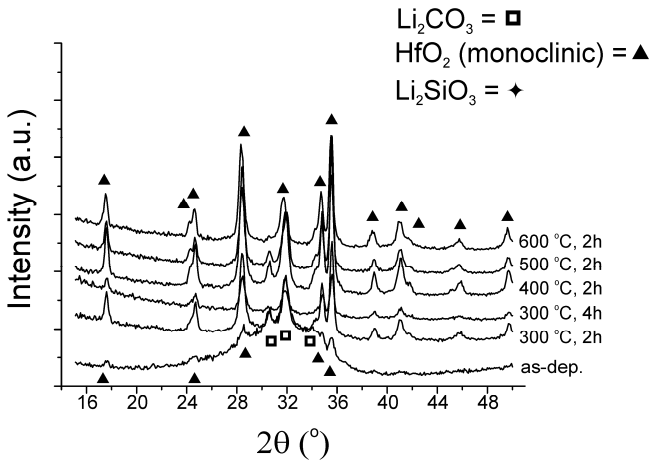

FIG. 6. X-ray diffractograms of a 3000 cycle Li_2CO_3 film deposited onto 50 nm HfO_2 and measured as-deposited and after annealing in air at various temperatures. Patterns: Li_2CO_3 = PDF 22–1141, JCPDS-ICDD, HfO_2 = PDF 34–0104, JCPDS-ICDD, Li_2SiO_3 = PDF 29–0828, JCPDS-ICDD.

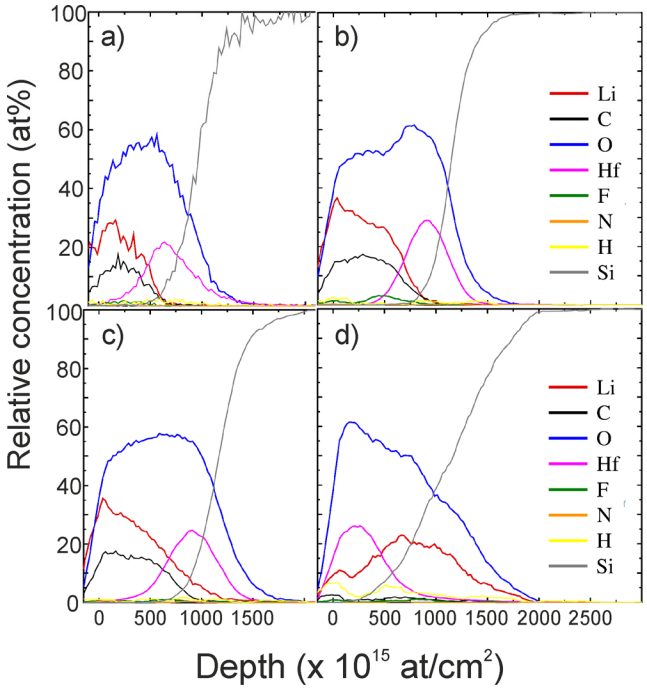

FIG. 7. ToF-ERDA depth profiles of a Li_2CO_3/HfO_2 film stack after annealing in air at 300 °C for 4 hours (a), 400 °C for 2 hours (b), 500 °C for 2 hours (c) and 600 °C for 2 hours (d).

With these experiments we were able to demonstrate that at elevated temperatures lithium ions can move through the well-known insulating material HfO_2 and react with the underlying silicon dioxide and silicon. To show that the reaction is not only limited to the formation of lithium silicates, a sample shown in Figure 8 was prepared. 3000 cycles of Li_2CO_3 was deposited onto 50 nm of HfO_2, which had been deposited onto approximately 60 nm of TiO_2. The TiO_2 film was deposited using titanium(IV) *iso*-propoxide and water. The three-layer stack was annealed in air at 650 °C for 30 minutes, and 2 and 4 hours. The X-ray diffractograms (Figure 9) show that already after 30 minutes of annealing, the lithium ions had diffused through the hafnia into the TiO_2 layer, forming crystalline Li_2TiO_3. Some anatase is also present in this layer, based both on Figure 9 and the metal ratio Li : Ti = 1.4 : 1, measured with ToF-ERDA. Again, the HfO_2 stays monoclinic before and after the annealing. Notably, no lithium silicate phases are detected with XRD. ToF-ERDA depth profiles corroborate the diffraction results by showing that after the annealing lithium is confined to the same layer together with titanium (Figure 10). In addition, both the depth profile and the FESEM image of the annealed film reveal that the hafnia and titania layers have not mixed, but remain separate despite the lithium diffusion (Figures 8 and 10).

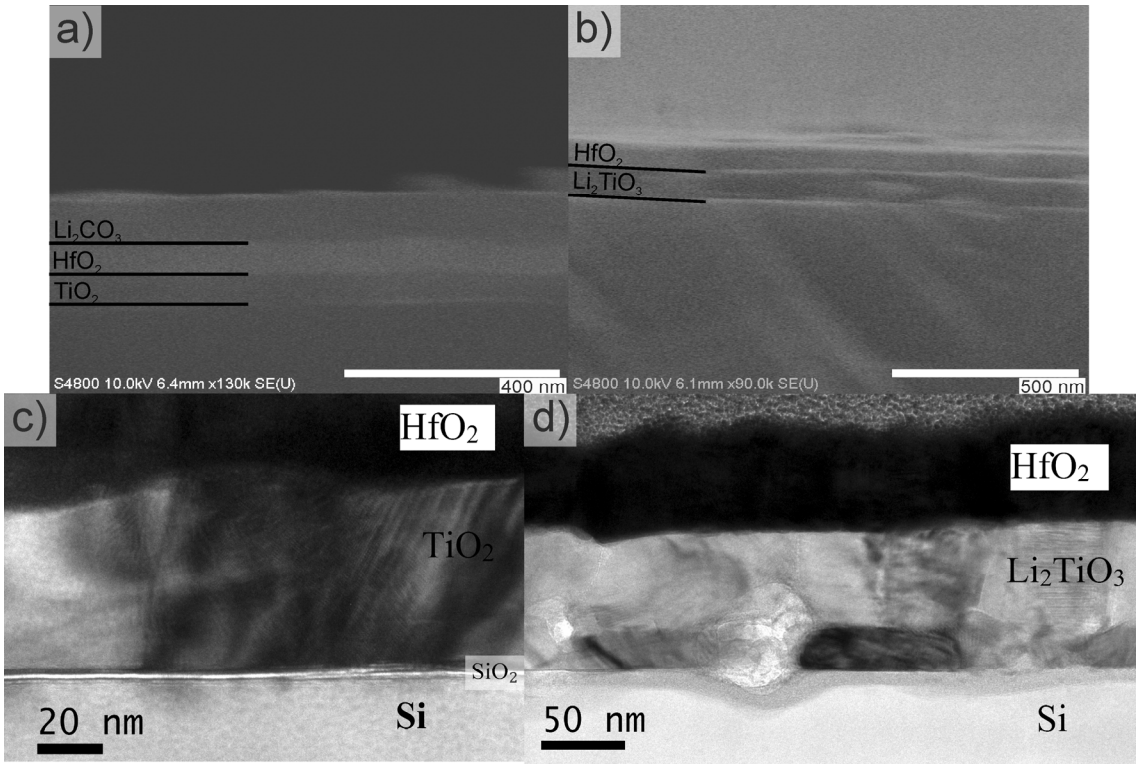

FIG. 8. FESEM and TEM images of a film stack composed of Li_2CO_3, HfO_2 and TiO_2 before (FESEM: a, TEM: c) and after annealing at 650 °C for 4 hours in air (FESEM: b, TEM: d). After the annealing only two layers remain.

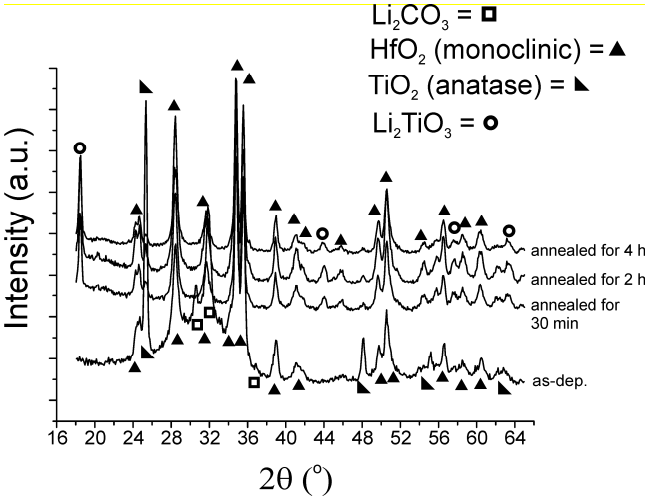

FIG. 9. X-ray diffractograms of a $Li_2CO_3/HfO_2/TiO_2$ stack before and after annealing at 650 °C in air. Patterns: Li_2CO_3 = PDF 22–1141, JCPDS-ICDD, HfO_2 = PDF 34–0104,

JCPDS-ICDD, TiO_2 = PDF 21–1272, JCPDS-ICDD, Li_2TiO_3 = PDF 33–0831, JCPDS-ICDD

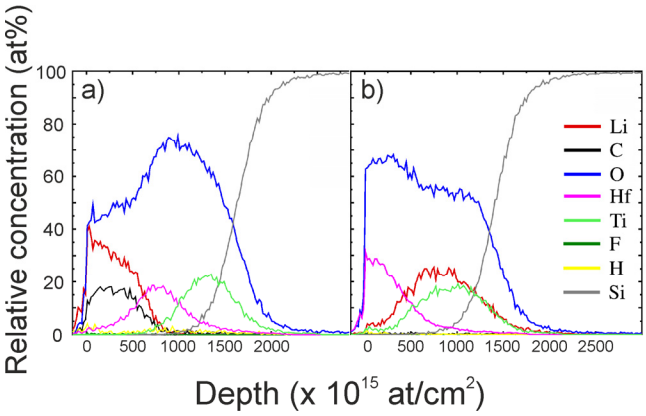

FIG. 10. ToF-ERDA depth profiles of a $Li_2CO_3/HfO_2/TiO_2$ stack before (a) and after annealing at 650 °C for 2 h in air (b).

The formation of the Li_2TiO_3 layer was also studied with TEM (Figure 8 c and d). Prior to the annealing of the $Li_2CO_3/HfO_2/TiO_2$ film stack, a native silicon oxide layer is present in the TiO_2/Si interface (Fig. 8 c). The anatase layer is comprised of a single layer of columnar grains. Several structural changes are observed in the annealed specimen (Fig. 8 d). Upon annealing, the apparent HfO_2 layer thickness increases from 50 to ca. 58 nm. This can be at least in part explained by the increased roughness of both the layer surface and the HfO_2/Li_2TiO_3 interface. It is noteworthy that the HfO_2 layer remains continuous, with no cracking or strong mixing with the Li_2TiO_3 layer taking place. In the TEM image taken after the annealing step, the Li_2TiO_3 layer thickness is in the range of 80–89 nm, as measured from individual spots along the cross-section, corresponding to ca. 50 % volume expansion compared to the original TiO_2 layer. This is consistent with the expected molar volume expansion upon conversion of anatase TiO_2 to Li_2TiO_3. The Li_2TiO_3 layer has two distinct grain heights, a thicker layer with ca. 60 nm tall grains in contact with the HfO_2 layer, and a lower ca 25 nm layer in contact with the Si interface. This can be due to the disappearance of the native SiO_2 layer, part of which may have

been incorporated into the lower part of the Li_2TiO_3 layer. A 10–15 nm reaction layer, possibly lithium doped Si or amorphous Li silicate, can be seen in the Li_2TiO_3, with some isolated grains of material which have grown through the mostly smooth Li_2TiO_3/Si interface layer.

B. ZrO_2 films as substrates

Similarly to the study on HfO_2, 3000 cycles of Li_2CO_3 was deposited onto a 54 nm ZrO_2 film at 225 °C, and the resulting film stack was annealed at various temperatures in air for 2 hours. The X-ray diffractogram (Figure 11) shows that at 500 °C some Li_2CO_3 is still present in the film stack. However, at 650 °C lithium has moved through the ZrO_2 film, forming silicates with silicon from the single-crystalline silicon substrate. At the same time, ZrO_2 has changed from the tetragonal phase of the as-deposited film to a mixture of tetragonal and monoclinic phases. No lithium zirconate phases formed in these conditions.

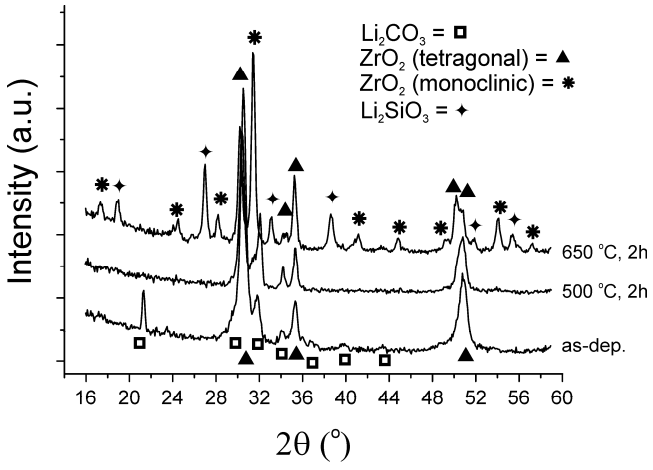

FIG. 11. X-ray diffractograms of a 3000 cycle Li_2CO_3 film deposited onto 54 nm ZrO_2 and measured as-deposited and after annealing in air at 500 and 650 °C. Patterns: Li_2CO_3 = PDF 22–1141, JCPDS-ICDD, ZrO_2 = Inorganic Crystal Structure Database (ICSD),

collection code 66781, and PDF 37–1484 JCPDS-ICDD, Li_2SiO_3 = PDF 29–0828, JCPDS-ICDD.

FESEM imaging was used to study the morphology of the Li_2CO_3/ZrO_2-stack before and after the annealing at 650 °C (Figure 12). The as-deposited film shows the same rough, flaky surface as in the case of Li_2CO_3 on the hafnium oxide films. After the annealing, the surface roughness is decreased dramatically, again similarly as on hafnia. However, the surface shows more defects and is also broken in some places (Fig. 12 c). The reason for this difference between hafnia and zirconia is difficult to explain. One possibility could be that the strain caused by lithium insertion is larger in the zirconia film. Another possibility is that during the annealing impurities such as hydroxyls are leaving the zirconia film, causing crater formation and cracks. HfO_2 films deposited using TEMAH and water have been reported to contain only very minor amounts of carbon and hydrogen impurities,[1] making crater formation less likely in this material. To study this problem further, we also imagined an annealed ZrO_2 film without Li_2CO_3 deposition. This film did not show similar cracking (not shown here), indicating that impurities in ZrO_2 most likely do not completely explain the cracking of the film. It appears that lithium plays a part in the changes in the morphology of the annealed stack.

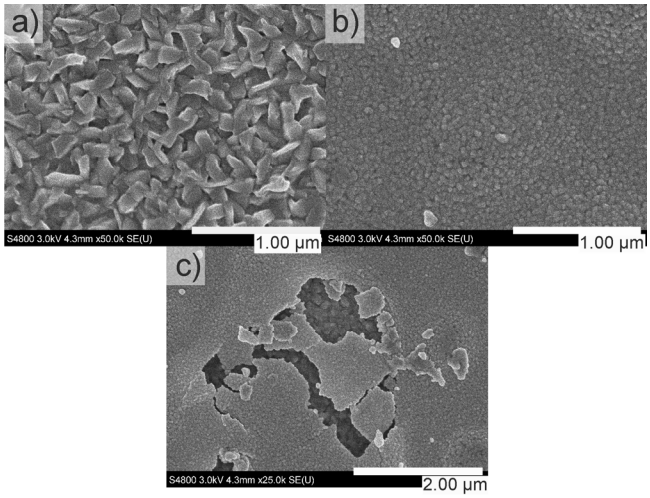

FIG. 12. FESEM images of 3000 cycles of Li_2CO_3 deposited by ALD onto 54 nm of ZrO_2, before (a) and after (b and c) annealing in air at 650 °C.

ToF-ERDA results (Table II) show that Li_2CO_3 forms close to stoichiometric onto ZrO_2. Most likely the slight deviation from stoichiometry is caused by the calculation not taking into account carbon impurities in the ZrO_2 film, which were measured to be of the order of 2.4 at% before annealing. It is apparent from Table II that annealing the film stack at 500 °C for 2 hours is not enough to remove the carbon and hydrogen impurities and to cause lithium migration. However, after annealing at 650 °C the lithium migration has taken place, with carbon and hydrogen impurities decreasing at the same time. The reaction is evident also in the ToF-ERDA depth profiles (Figure 13). Lithium has moved into the silicon substrate after annealing at 650 °C, while at the lower annealing temperature the profile for the most part resembles that of the as-deposited sample. The depth profile of the as-deposited sample also revealed that most of the hydrogen

impurities reside in the zirconia layer. Despite being embedded in this bottom layer, these impurities can be removed with annealing.

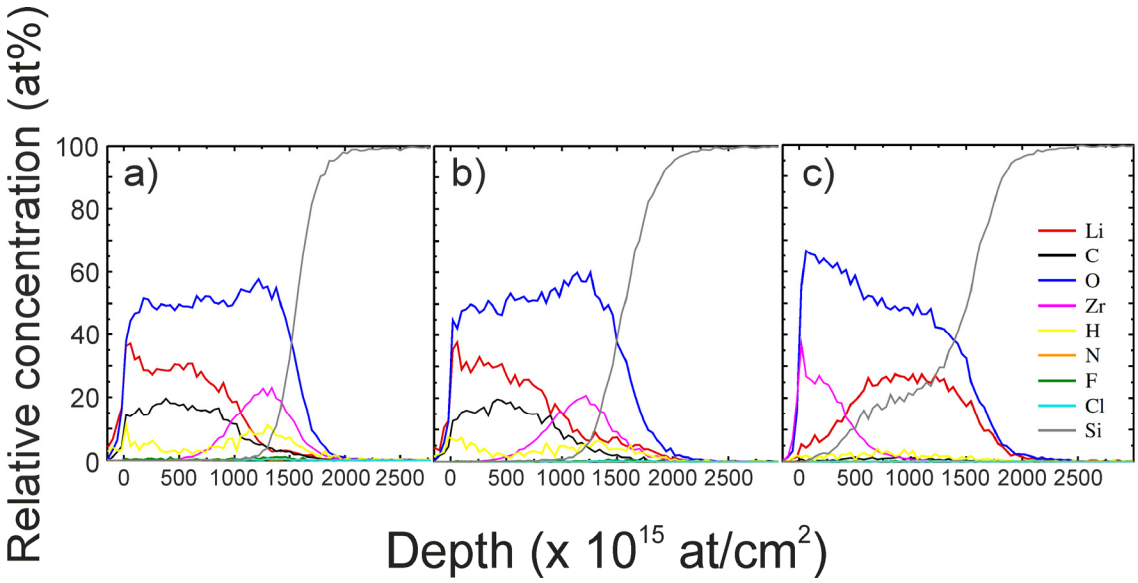

FIG. 13. ToF-ERDA depth profiles of a Li_2CO_3/ZrO_2 film stack as-deposited (a) and after annealing at 500 °C (b) and 650 °C (c) for 2 hours in air.

TABLE II. ToF-ERDA results (at%) of a 3000 cycle Li_2CO_3 film deposited onto 54 nm ZrO_2 and measured as-deposited and after annealing at 500 °C and 650 °C for 2 h in air.

	Li_2CO_3 / ZrO_2 as-deposited	**Li_2CO_3 / ZrO_2 after anneal at 500 °C**	**Li_2CO_3 / ZrO_2 after anneal at 650 °C**
Li	19.7±1.0	20.2±1.1	25.7±1.3
Zr	9.4±0.3	9.3±0.3	9.3±0.3
O	52.0±1.0	54.3±1.1	61.2±1.2
C	11.9±0.5	11.4±0.6	0.93±0.15
H	6.2±0.9	4.5±0.7	2.5±0.6
F	0.50±0.09	0.21±0.06	0.09±0.04
Cl	0.13±0.04	0.06±0.03	0.07±0.03
N	0.13±0.05	0.11±0.05	0.09±0.05
Elemental ratios	Assuming stoichiometric ZrO_2: Li:C:O = 1.7 : 1 : 2.8	Li : Zr : O = 2.2 : 1 : 5.8	Li : Zr : O = 2.8 : 1 : 6.6

Based on these results it is clear that hafnium and zirconium oxides behave quite similarly when annealed with a lithium carbonate film on top. This is somewhat surprising considering the large amount of literature on lithium zirconates: one could assume that producing lithium zirconates with solid state reactions would be more straightforward than obtaining lithium hafnates. To still study whether we could synthesize lithium zirconates with this solid state reaction process, a thinner ZrO_2 film of 30 nm was used, together with 3000 cycles of Li_2CO_3. The idea behind this experiment was to drive lithium into the thinner zirconia layer at a lower temperature than above so

that lithium would not react with the substrate but instead with zirconia, producing a crystalline lithium zirconate. Figure 14 shows a ToF-ERDA depth profile and an X-ray diffractogram of a film stack deposited at 225 °C and annealed at 500 °C. It is evident that with the thinner zirconia film, lithium mixing occurs throughout the film already after annealing at 500 °C. This has to do with the smaller thickness of the zirconia film promoting faster lithium diffusion. At 500 °C our previous sample was tetragonal, whereas the thinner sample showed peaks belonging to both tetragonal and monoclinic zirconia, which might also mean that the ionic conductivity is different in this sample. In any case, it is evident that only crystalline ZrO_2 is present in the diffractogram of the annealed sample. The atomic percentages in the annealed film, as determined by ToF-ERDA, were: Li 25,3, Zr 7.2, O 53.7, C 5.8, H 7.3, F 0.6 and N 0.1. The excess oxygen is most likely in the form of lithium carbonate, since not all carbon has been removed at this temperature. Based on these results, the closest lithium zirconate phase possible would be either Li_2ZrO_3 or $Li_6Zr_2O_7$. However, the phase cannot be unambiguously be recognized in the X-ray diffractogram in Figure 14b. Still, the small, broad peak at 22.1–22.9 ° (2θ) could originate from a zirconate phase.[26–28] Further identification of the phase was impossible at this time, which is why we believe that making lithium zirconate films with this process is not feasible.

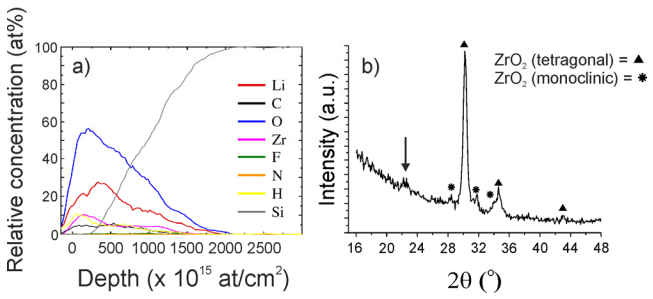

FIG. 14. ToF-ERDA depth profile (a) and X-ray diffractogram (b) of a Li_2CO_3/ZrO_2 film stack after annealing at 500 °C for 2 h in air. The ZrO_2 film thickness was 30 nm and Li_2CO_3 was applied for 3000 cycles. Patterns: ZrO_2 = Inorganic Crystal Structure Database (ICSD), collection code 66781, and PDF 37–1484 JCPDS-ICDD.

It has been reported that forming Li_2ZrO_3 from either LiOH or Li_2CO_3 and ZrO_2 using solid state reactions involves much higher temperatures than, for example, in the case of Li_2TiO_3.[14,29] Therefore, we are faced with a similar problem with Li_2ZrO_3 as we were previously with producing $Li_4Ti_5O_{12}$:[6] the temperature range available for our system is limited due to lithium reactivity with silicon. The chemical potential of lithium silicate formation appears to drive the lithium migration though the zirconium oxide layer to the interface with the substrate before any reaction with the zirconia can occur.

IV. SUMMARY AND CONCLUSIONS

In this paper, we have studied the reactions between atomic layer deposited Li_2CO_3 and HfO_2 or ZrO_2. After annealing the films at 650 °C, lithium silicates have formed with no indication of lithium hafnate or zirconate phases. Thus, it appears that these materials behave differently from TiO_2, Ta_2O_5 and Nb_2O_5, which we have studied

previously and found to form lithium containing ternary phases.[6] After annealing the films showed a relatively smooth surface with some defects. We postulate that these defects are formed when impurities are removed from the metal oxide layer and when lithium is inserted into the silicon substrate. Next, more research should be done on both the amorphous phases and the different crystalline phases of HfO_2 and ZrO_2, as the phase could have a large effect on the lithium diffusivity.[5] In addition, further attempts to deposit Li_2ZrO_3 should be made using a lithium diffusion barrier under the ZrO_2 layer, as Li_2ZrO_3 could also prove to be a useful lithium-ion battery material.

ACKNOWLEDGMENTS

The authors would like to thank the electron microscopy unit of the Institute of Biotechnology at the University of Helsinki for providing TEM instrument access.

Mrs. Sanni Seppälä is thanked for the ZrO_2 depositions.

Financial support from ASM Microchemistry Oy is gratefully acknowledged. This work was also supported by the Finnish Centre of Excellence in Atomic Layer Deposition.

[1]K. Kukli, M. Ritala, T. Sajavaara, J. Keinonen, and M. Leskelä, Chem. Vap. Deposition **8** 199 (2002).

[2]V. A. Gritsenko, T. V. Perevalov, and D. R. Islamov, Phys. Rep. **613,** 1 (2016).

[3]H. Xia, H. L. Wang, W. Xiao, M. O. Lai, and L. Lu, Int. J. Surf. Sci. Eng. **3**, 23 (2009).

[4]N. Yesibolati, M. Shahid, W. Chen, M. N. Hedhili, M. C. Reuter, F. M. Ross, and H. N. Alshareef, Small **10**, 2849 (2014).

[5]A. K. Jonsson, G. A. Niklasson, M. Ritala, M. Leskelä, and K. Kukli, J. Electrochem. Soc. **151**, F54 (2004).

[6]E. Atosuo, M. Mäntymäki, K. Mizohata, M. J. Heikkilä, J. Räisänen, M. Ritala, and M. Leskelä, Chem. Mater. **29**, 998 (2017).

[7]PDF 23–1183, JCPDS-ICDD, International Center for Diffraction Data.

[8]PDF 26–0847, JCPDS-ICDD, International Center for Diffraction Data.

[9]Ya. V. Baklanova, A. V. Ishchenko, T. A. Denisova, L. G. Maksimova, B. V. Shulgin, V. A. Pustovarov, and L. V. Viktorov, Opt. Mater. **34**, 1037 (2012).

[10]R. Czekalla and W. Jeitschko, Z. Anorg. Allg. Chem. **619**, 2038 (1993).

[11]Z. Miao, H. Ni, H. Zhang, C. Wang, J. Fang, and G. Yang, J. Power Sources **264**, 147 (2014).

[12]Y. Xu, Y. Liu, Z. Lu, H. Wang, D. Sun, and G. Yang, Appl. Surf. Sci. **361**, 150 (2016).

[13]Y. Dong, Y. Zhao, H. Duan, and J. Huang, Electrochim. Acta **161**, 219 (2015).

[14]D. Cruz, H. Pfeiffer, and S. Bulbulian, Solid State Sci. **8**, 470 (2006).

[15]S. Huang, B. E. Wilson, B. Wang, Y. Fang, K. Buffington, A. Stein, and D. G. Truhlar, J. Am. Chem. Soc. **137**, 10992 (2015).

[16]S. Huang, B. E. Wilson, W. H. Smyrl, D. G. Truhlar, and A. Stein, Chem. Mater. **28**, 746 (2016).

[17]S. Seppälä, unpublished results.

[18]M. Putkonen, T. Aaltonen, M. Alnes, T. Sajavaara, O. Nilsen, and H. Fjellvåg, J. Mater. Chem. **19**, 8767 (2009).

[19]J. Jokinen, J. Keinonen, P. Tikkanen, A. Kuronen, T. Ahlgren, and K. Nordlund, Nucl. Instr. and Meth. B **119**, 533 (1996).

[20]PDF 34–1416, JCPDS-ICDD, International Center for Diffraction Data.

[21]M.-Y. Ho, H. Gong, G. D. Wilk, B. W. Busch, M. L. Green, P. M. Voyles, D. A. Muller, M. Bude, W. H. Lin, A. See, M. E. Loomans, S. K. Lahiri, and P. I. Räisänen, J. Appl. Phys. **93**, 1477 (2003).

[22]S. Ferrari and G. Scarel, J. Appl. Phys. **96**, 144 (2004).

[23]G. He, M. Liu, L. Q. Zhu, M. Chang, Q. Fang, and L. D. Zhang, Surf. Sci. **576**, 67 (2005).

[24]E. Østreng, H. H. Sønsteby, T. Sajavaara, O. Nilsen, and H. Fjellvåg, J. Mater. Chem. C **1**, 4283 (2013).

[25]V. Miikkulainen, O. Nilsen, M. Laitinen, T. Sajavaara, and H. Fjellvåg, RSC Adv. **3** 7537 (2013).

[26]PDF 33–0843, JCPDS-ICDD, International Center for Diffraction Data.

[27]Inorganic Crystal Structure Database (ICSD), collection code 41321.

[28]Inorganic Crystal Structure Database (ICSD), collection code 73835.

[29]J. Ida, R. Xiong, and Y. S. Lin, Sep. Purif. Technol. **36**, 41 (2004).